Malic Enzyme Facilitates d-Lactate Production through Increased Pyruvate Supply during Anoxic Dark Fermentation in Synechocystis sp. PCC 6803

Hidese, Ryota
Matsuda, Mami
Osanai, Takashi
Hasunuma, Tomohisa
Kondo, Akihiko

(Citation)
ACS Synthetic Biology,9(2):260-268

(Issue Date)
2020-01-31

(Resource Type)
journal article

(Version)
Accepted Manuscript

Malic enzyme facilitates D-lactate production through increased pyruvate supply during anoxic dark fermentation in *Synechocystis sp.* PCC 6803

Ryota Hidese[a#], Mami Matsuda[a,b#], Takashi Osanai[c], Tomohisa Hasunuma[a,b*], and Akihiko Kondo[a,b,d].

[a]Graduate School of Science, Innovation and Technology, Kobe University, 1-1 Rokkodai, Nada, Kobe 657-8501, Japan. [b]Engineering Biology Research Center, Kobe University, 1-1 Rokkodai, Nada, Kobe, Hyogo 657-8501, Japan. [c]School of Agriculture, Meiji University, 1-1-1 Higashimita, Tama-ku, Kawasaki, Kanagawa 214-8571, Japan. [d]Biomass Engineering Program, RIKEN, 1-7-22 Suehiro, Tsurumi, Yokohama, Kanagawa 230-0045, Japan

#The authors were equally contributed.

*Corresponding author: Tomohisa Hasunuma

Engineering Biology Research Center, Kobe University, 1-1 Rokkodai, Nada, Kobe 657-8501, Japan

Tel: +81-78-803-6356; Fax: +81-78-803-6192

E-mail: hasunuma@port.kobe-u.ac.jp

Key words:

Cyanobacteria; D-Lactate; Malate dehydrogenase (decarboxylating); Metabolomics; *Synechocystis* sp. PCC6803

Abstract

D-Lactate is one of the most valuable compounds for manufacturing bio-based polymers. Here, we have investigated the significance of endogenous malate dehydrogenase (decarboxylating) (Malic enzyme, ME), which catalyzes the oxidative decarboxylation of malate to pyruvate, in D-lactate biosynthesis in the cyanobacterium *Synechocystis* sp. PCC6803. D-Lactate levels were increased by two-fold in ME-overexpressing strains, while levels in ME-deficient strains were almost equivalent to those in the host strain. Dynamic metabolomics revealed that overexpression of ME led to increased turnover rates in malate and pyruvate metabolism; in contrast, deletion of ME resulted in increased pool sizes of glycolytic intermediates, probably due to sequential feedback inhibition, initially triggered by malate accumulation. Finally, both the loss of the acetate kinase gene and overexpression of endogenous D-lactate dehydrogenase, concurrent with ME overexpression, resulted in the highest production of D-lactate (26.6 g/L) with an initial cell concentration of 75 g-DCW/L after 72 h fermentation.

Bio-based polymers, defined as polymers produced from renewable biological resources, play a key role in building a sustainable bioeconomy. Poly(lactic acid) (PLA), which is one of the major bio-based polymers composed of lactate, is widely used as a biodegradable polyester[1,2]. Stereocomplex PLA is formed by blending enantiomeric PLAs, poly(L-lactide) and poly(D-lactide), and prominently exhibits enhanced mechanical properties as well as heat and hydrolysis resistance[3,4]. The large-scale industrial production of optically pure L-lactate has been accomplished by fermentation using *Lactobacillus* and *Bacillus* strains[5,6]. On the other hand, biorefineries demand the availability of optically pure D-lactate, an issue that remains to be resolved.

Algae-based biorefinement is a promising technology that is expected to contribute to a sustainable low-carbon future[7-11]. Cyanobacteria are photosynthetic organisms capable of generating organic compounds from carbon dioxide through oxygenic photosynthesis, and have attracted considerable attention as a host organism for the production of valuable chemicals and biofuels including alcohols, diols, hydrocarbons, and organic acids[9,10,12-15]. In particular, *Synechocystis* sp. PCC 6803 (hereafter *Synechocystis* 6803) is a unicellular and non-nitrogen fixing cyanobacterium, which is well-characterized in terms of physiology, biochemistry, and genetics. Furthermore, advances in genetic engineering of *Synechocystis* 6803 have enabled successful improvement of photosynthetic activity and metabolic engineering toward the production of a variety of chemicals.

Synechocystis 6803 accumulates the storage polysaccharide glycogen from carbon dioxide during oxygenic photosynthesis, and then catabolizes the stored carbohydrate molecule via autofermentation under dark anoxic conditions[16]. In such conditions, *Synechocystis* 6803 excretes hydrogen, carbon dioxide, and a variety of organic acids including acetate, formate, succinate, and D-lactate[16-18]. Our previous dynamic metabolomics combined *in vivo* ^{13}C labeling of metabolites and metabolomics, thereby allowing kinetic visualization of carbon metabolism and identification of the limiting steps in central metabolic pathways[19]. This enabled the identification of the primary biosynthetic pathway of succinate from glycogen via glycolysis, the pentose phosphate pathway, the anaplerotic pathway, and the reductive TCA cycle, called the reductive branch of the TCA cycle[20]. This study also reported the increased intracellular levels of malate, fumarate, and succinate, suggesting that utilization of carbon flux in the reductive TCA cycle would be a key factor toward D-lactate production (Fig. 1). D-Lactate is biosynthesized from pyruvate by D-lactate dehydrogenase (*slr1556*, *Sy*Ddh) using NADH and NADPH as cofactors under fermentation[21]. Malate dehydrogenase (decarboxylating) (Malic enzyme, ME) [EC: 1.1.1.39], catalyzes the oxidative decarboxylation of malate to pyruvate using $NADP^+$ as a specific cofactor[22]; however, the roles of ME in central metabolism under autofermentation remain unknown.

In the present study, we analyzed the D-lactate production of *Synechocystis* 6803, ME-deficient (ΔME strain) and ME-overexpressing strains (ME-ox strain) and compared metabolite pool sizes and fluxes of glycolysis and the reductive TCA cycle among the strains to determine the reaction

limiting the conversion of storage glycogen to D-lactate biosynthesis. Furthermore, the highest production of D-lactate was achieved by both overexpression of *Sy*Ddh and disruption of the *ackA* (*sll1299*) gene, which encodes the acetate kinase responsible for acetate production, in combination with ME overexpression.

Results

Effect of malate dehydrogenase (decarboxylating) overexpression on organic acid production

The glucose-tolerant (GT) strain *Synechocystis* sp. PCC6803[23], which is adapted to utilize glucose as a carbon source, was used as the host strain. To overexpress the endogenous ME gene under the control of the constitutive promoter *trc*, the gene was introduced by homologous recombination into a neutral site, *slr0168*, of the *Synechocystis* 6803 genome (Supplementary Fig. S1 in the Supporting Information). A control strain (CT) was constructed by the integration of the kanamycin resistant gene tandemly arranged with the *trc* promoter region into the *slr0618* loci. The *me* gene was disrupted by integrating the kanamycin resistant gene tandemly arranged with the *psbA2* promoter region into the *slr0721* loci (Supplementary Fig. S1).

The recombinant *Synechocystis* 6803 strains were cultivated for 3 days under photoautotrophic conditions at 30 °C, and fermentation at initial cell concentration of 5 g-DCW/L was then carried out to initiate organic acid secretion under dark anoxic conditions for 96 hours at 37 °C (Fig. 2). The extracellular organic acids were analyzed by HPLC. The concentration of D-lactate in the ME-ox strain (364.4 mg/L) was two-fold higher than that of the CT strain (181.4 mg/L), while the concentration in the ΔME strain (154.6 mg/L) was quantitatively decreased compared to that of the CT strain. The initial glycogen contents before fermentation were comparable among those strains (approximately 40%). The glycogen content of the ME-ox strain (15.5%) was quantitatively lower than that of the CT strain (17.0%); however, the ΔME strain exhibited substantially lower glycogen content (4.2%) compared to that of CT strain. Next, the production of acetate and succinate was analyzed because these metabolites are produced and secreted concomitantly with intracellular glycogen consumption during autofermentation. Overexpression of ME resulted in a < 1.2-fold decrease in acetate and succinate levels. In contrast, disruption of the *me* gene substantially increased the acetate concentration (2116.1 mg/L) compared to that of the CT strain (1650.8 mg/L). Under dark anoxic conditions, succinate is biosynthesized through the reductive TCA cycle. Succinate concentrations of both the ME-ox (176.6 mg/L) and ΔME strains (167.7 mg/L) were lower than that of the CT strain (205.9 mg/L).

Metabolome and ^{13}C-metabolic turnover analyses

Intracellular metabolites were extracted from the recombinant *Synechocystis* 6803 cells after 3, 6, 24, 48, 72, and 96 h fermentation. The pool sizes of hexose phosphates (glucose-6-phosphate, G6P;

fructose-6-phosphate, F6P; fructose-1,6-bisphosphate, FBP), triose phosphates (3-phosphoglycerate, 3PGA; phosphoenolpyruvate, PEP), organic acids (pyruvate, lactate, malate, fumarate, succinate, and citrate), and acetyl-CoA were obtained by calculating their respective peak areas from capillary electrophoresis-mass spectrometry (CE-MS) analysis (Fig. 3). The pool sizes of G6P, F6P, and FBP in the ΔME cells were significantly higher than those in the CT and ME-ox cells during 0-48 h fermentation. The ΔME cells accumulated large amounts of 3PGA (5.7 μmol/g-DCW), PEP (1.9 μmol/g-DCW), malate (13.0 μmol/g-DCW), fumarate (2.8 μmol/g-DCW), and succinate (8.2 μmol/g-DCW) during the first 6 h fermentation compared to those in the ME-ox and CT cells. In addition, malate and fumarate in the ME-ox and CT cells peaked at 24 h fermentation. The peak increase in the pool size of citrate (6.1 μmol/g-DCW) observed in the ME-ox cells occurred after 24 h fermentation; whereas the peak pool sizes in the ΔME and CT cells were 3.2- and 2.8-μmol/g-DCW, observed during the first 3 and 6 h fermentation, respectively. Accumulation of pyruvate was observed in the ΔME cells after 96 h fermentation, with the pool size peaking at 0.1 μmol/g-DCW; however, the pools size of acetyl-CoA was significantly lower than those of the ME-ox and CT cells. The pool sizes of PEP, malate, fumarate, and succinate in the ME-ox strain were quantitatively (0.75-, 0.47-, 0.49-, and 0.76-fold, respectively) lower than those in the CT strain after 6 h fermentation. Low FBP abundance in the ME-ox cells was observed during fermentation compared to CT cells. On the other hand, intracellular lactate levels were comparable among the CT, ME-ox and ΔME strains. Oxaloacetate was not detected with the present mass spectrometry due to its low abundance.

Next, ^{13}C-labeling was performed to visualize the turnover of metabolic intermediates in the recombinant *Synechocystis* 6803 strains. ^{13}C was incorporated into organic acids in the cyanobacteria cells through the carboxylase family of enzymes, such as PEP carboxylase, following the addition of $NaH^{13}CO_3$ as a substrate to cells inoculated into 0.1 M Hepes-KOH, pH 7.8 (Fig. 4). The ^{13}C fraction, defined as the ratio of ^{13}C to the total carbon of each metabolite, was calculated from the mass isotopomer distributions. As a result, the ^{13}C fractions of PEP and lactate were observed to gradually increase during 48 h cultivation of the CT, ME-ox, and ΔME strains. The ^{13}C fraction of citrate reached about 20% within 1 h of labeling. The ^{13}C fractions of malate, fumarate, and succinate reached a maximum within 4-6 h of labeling in the ME-ox strain, with the ^{13}C fractions of malate and fumarate being higher than in the CT strain during cultivation. In contrast, levels in the ΔME strain were significantly lower than in the CT strain during 0-6 h cultivation. Also, the ME-ox strain showed high ^{13}C enrichment of succinate compared to the CT and ΔME strains during 0-4 h cultivation, even though the maximum ^{13}C fractions were comparable among the three strains. The ^{13}C incorporation of malate, fumarate, and lactate in the ME-ox cells, with a maximum of about 33%, 33%, and 15%, respectively, was significantly higher than those in the CT and ΔME cells. On the other hand, the ^{13}C fraction of PEP in the ME-ox cells reached a maximum of 8% after

48 h of labeling, and was lower than in the other strains. The ^{13}C-enrichment pattern of citrate was comparable among the three strains. The ^{13}C fractions of pyruvate and acetyl-CoA were too low to calculate. These data clearly indicated that D-lactate is biosynthesized via the anaplerotic pathway involving phosphoenolpyruvate carboxylase, ME and D-lactate dehydrogenase.

Enhancement of D-lactate production by disruption of *ackA* and overexpression of *ddh*

As shown in Fig. 1, the acetate concentration was more than 1500 mg/L even in the ME-ox strain, whose lactate production was about 364 mg/L. Given the D-lactate production is often inversely proportional to the acetate production, we carried out the deletion of endogenous *ackA* (*sll1299*) encoding acetate kinase and overexpression of endogenous *ddh* (*slr1556*) encoding D-lactate dehydrogenase, under the control of a strong constitutive promoter (*psbA2*), in the host strain ME-ox (Supplementary Fig. S1). The *ackA* gene in the ME-ox strain was disrupted by introducing a cassette including the chloramphenicol resistance gene to yield the strain ME-ox/ΔackA. The recombinant strain ME-ox/ΔackA/ddh-ox was constructed by integrating a cassette containing the *ddh* gene under the *psbA2* promoter into the loci of the *ackA* gene in the ME-ox strain. Complete segregation was confirmed by genomic PCR (Supplementary Fig. S1).

ME-ox/ΔackA/ddh-ox and ME-ox/ΔackA were cultivated for 3 days under photoautotrophic conditions, and fermentation was performed at 37 °C for 24 h in 0.1 M Hepes-KOH (pH 7.8) containing 300 mM $NaHCO_3$. The D-lactate dehydrogenase activity of the ME-ox/ΔackA/ddh-ox cells (294.1 ± 10.7 U/g-protein) was about 18-fold higher than that of the ME-ox/ΔackA cells (16.4 ± 2.5 U/g-protein) ($P < 0.01$, student's *t*-test). Next, we profiled time-course changes in organic acid production of the recombinant strains. As expected, the deletion of *ackA* resulted in a significant decrease in acetate concentration and an increase in D-lactate concentration (Fig. 5), since pyruvate is a precursor for both D-lactate and acetate biosynthesis. Moreover, overexpression of the *ddh* gene contributed to the increased production of D-lactate. In contrast, the succinate concentrations were similar between strains.

Finally, we investigated the effect of initial cell concentration of the ME-ox/ΔackA/ddh-ox strain on the production of organic acids. The recombinant cells were cultivated for 3 days under photoautotrophic conditions and harvested at the logarithmic phase (approximately 1.5 g-DCW/L). The harvested cells were inoculated to 10 mL of 0.1 M Hepes-KOH (pH 7.8) at each initial cell concentration (5, 12.5, 25, 50, and 75 g-DCW/L). Production of D-lactate, acetate, and succinate was estimated following fermentation with 300 mM $NaHCO_3$ at different initial concentrations. Addition of 300 mM $NaHCO_3$ promotes intracellular glycogen metabolism in fermentation[20]. The D-lactate and acetate concentrations after 72 h fermentation were increased in an initial cell concentration-dependent manner (Fig. 6). The D-lactate concentration (1.35 g/L) was found after 3 days fermentation at 5 g-DCW/L condition (0.270 g D-lactate/g-DCW). On the other hand, the

specific D-lactate yield peaked at 25 g-DCW/L condition (0.386 g D-lactate /g-DCW) (Fig. 6). The highest production (26.6 g/L) of D-lactate was achieved at 75 g-DCW/L condition and the initial glucose concentration (29.6 g/L) before fermentation decreased to 1.4 g/L of that after 72 h fermentation. The volumetric D-lactate yield was 94.3% (g D-lactate/g glucose). In contrast, the specific acetate yield peaked at 75 g-DCW/L condition. The succinate levels were comparable among the 25, 50, and 75 g-DCW/L (about 0.4 g/L) conditions, but the specific succinate yield decreased with increasing the initial cell density from 25 g-DCW/L to 75 g-DCW/L.

Discussion

In the present study, we analyzed the metabolic pool sizes and ^{13}C-metabolic turnover of ΔME and ME-ox strains cultivated under dark anoxic conditions, revealing differences in the dynamic metabolomics of glycolysis and pyruvate metabolism in response to the absence or overexpression of ME. The present study clarifies novel aspects of the physiological functions of ME. Previous ^{13}C-metabolic flux analysis using [^{13}C-U] glucose revealed that ME is responsible for the substantial outflow toward pyruvate biosynthesis in photomixotrophic, photoautotrophic, and dark heterotrophic conditions[24,25]. It is well known that the *Synechocystis* 6803 mutant, which carries a transposon insertional mutation in the *me* gene, grows well under photomixotrophic cultivation on glucose or diurnal light conditions (12 h light and 12 h dark), while showing poor photoautotrophic growth[22]. In addition, disruption of the *me* gene led to a severe growth defect under dark heterotrophic conditions[26]. The growth defect under photoautotrophic conditions, but not dark heterotrophic conditions, is restored by the addition of pyruvate[22,26]; that is, ME bypasses and compensates the pyruvate production by pyruvate kinase, which catalyzes the conversion of PEP to pyruvate, under continuous illumination conditions.

Intracellular glycogen consumption during autofermentation concomitantly occurs secretion of various organic acids including acetate, D-lactate, succinate, 2-ketoglutarate, malate, and fumarate[20]. In Fig. 1, the acetate concentration was increased in the ΔME strain, whose glycogen content is lower than that of the CT strain after 96 h fermentation. Low acetyl-CoA pool size would be due to high acetate production in ΔME strain (Fig. 3). The increased pool sizes of glycolytic intermediates (G6P, F6P, FBP, 3PGA, and PEP) in the ΔME cells is suggested to be caused by the accumulation of malate. Moreover, the increased pool size of pyruvate after 96 h fermentation would be attributed to the retardation of glycolysis (Fig. 3), probably reflecting the decreased pool sizes of G6P, F6P, and FBP at 96 h. The ^{13}C-labeled sodium bicarbonate is mostly incorporated into malate via oxaloacetate by the catalysis of PEP carboxylase[20], meanwhile, small $^{13}CO_2$ fixation by ribulose 1,5-bisphosphate carboxylase/oxygenase contributes to the ^{13}C-labeling of PEP via pentose phosphate pathway under dark anoxic condition[26]. The amount of ^{13}C-labeled PEP in ME-ox strain was significantly higher than that in CT strain at the early of fermentation (0 hr) (Fig. 4), implying high turnover of PEP in

ME-ox strain. We expect that accumulation of PEP in ΔME strain caused the slight increase of ^{13}C enrichment after 48h fermentation. Furthermore, it was recently reported that the citrate synthase of *Synechocystis* 6803 is unique, in that the inhibitors are not only citrate and 2-oxoglutarate but also PEP; however, NADH and ATP, which are typical inhibitors of bacterial citrate synthase, are not[27]. Overall, the carbon flux from glycogen is distributed to acetate production much more than the influx into the oxidative TCA cycle, probably due to sequential feedback inhibition initially caused by malate accumulation; that is, the increased amount of malate in ΔME strain resulted in the accumulation of PEP through the allosteric inhibition of pyruvate kinase activity[28], leading to non-competitive inhibition of citrate synthase activity. Low acetyl-CoA pool size would contribute to enhance the activity of pyruvate dehydrogenase complex, which catalyzes the irreversible conversion of pyruvate into acetyl-CoA[29]. Also, this metabolic feature, which is associated with ME-deletion, might be attributed to the growth defect under dark anoxic conditions.

Conversely, overexpression of ME contributed to D-lactate production through the pyruvate supply, based on our dynamic metabolomics. The overexpression promoted the ^{13}C-metabolic turnover of malate, fumarate, and succinate (Fig. 4), resulting in their small metabolic pool sizes after 6 h fermentation (Fig. 3) compared to those in CT strain. In contrast, the loss of ME caused the retardation of the reductive TCA pathway, as revealed by the dynamic metabolomics. Results of the metabolomics indicated that in addition to D-lactate production, citrate would be synthesized through the over-supply of pyruvate. Furthermore, the low abundance of malate would promote ^{13}C-metabolic turnover of PEP at the early of fermentation, leading to increased glycolytic flux into pyruvate.

Several studies have described the microbial production of D-lactate via engineering of the metabolic pathway in various heterotrophic organisms. These include *Bacillus* species[30-33], *E. coli* with the highest reported heterotrophic D-lactate concentration[34], *Saccharomyces cerevisiae*[35], in addition to the genetically modified bacteria *Sporolactobacillus inulins*[36] and *Lactobacillus* species[37,38]. In photoautotrophic organisms, pathway engineering approaches have focused on the enhancement of D-lactate production in *Synechocystis* 6803 and *Synechococcus elongatus* PCC7942: 1. Overexpression of either of the genes responsible for D-lactate, such as the mutated *Bacillus coagulans* glycerol dehydrogenase (Mutated GlyDH)[39,40] or an engineered NADPH-dependent D-lactate dehydrogenase (*Lm*LdhD) from *Leuconostoc mesenteroides*[41]; 2. Pathway knockout of acetyl-CoA metabolism through the disruption of genes for native poly-3-hydroxybutyrate biosynthesis (*phaCE*, *slr1829* and *slr1830*) and acetate biosynthetic pathways (*pta, slr0213*) in *Synechocystis* 6803[42]; 3. A new metabolic route from a glycolytic intermediate dihydroxyacetone phosphate to D-lactate via *s*-lactoylglutathione was conferred by introduction of exogenous methylglyoxal synthase gene (*mgsA*) and lactate/H^+ symporter (*lldP*), acting in concert with intrinsic GloAB enzymes in *S. elongatus* PCC7942[43]. However, the D-lactate concentrations of these

engineered cyanobacteria strains remain around 1 g/L (Table 1). The low productivity on photoautotrophic bioproduction is mainly attributed to low carbon flux to the TCA cycle and acetyl-CoA. Dark fermentation or nitrogen deprivation drives sufficient carbon flux to pyruvate and/or acetyl-CoA, however, nitrogen deprivation can result in decreased cell growth, thereby reducing overall product yields[15].

We previously reported that a high D-lactate concentration (10.7 g/L) was accomplished by autofermentation with an initial cell concentration of 50 g-DCW/L at 37 °C in recombinant *Synechocystis* 6803, which overexpresses the endogenous PEP carboxylase gene (*ppc, sll0920*) and lacks the *ackA* gene[44]. Thus, we have successfully demonstrated that fermentation has the advantage that it shorten cultivation time when compared to photoautotrophic condition, resulting in the increased D-lactate productivity. Considering succinate is biosynthesized through the reductive TCA cycle, engineering malate metabolism could facilitate D-lactate production. Our dynamic metabolomics presented here indicated that overexpression of ME is important for not only pyruvate supply, but also promoting glycolysis. These findings enabled further metabolic design toward D-lactate bioproduction. We successfully demonstrated that the combination of *ackA* gene disruption and *ddh* gene overexpression, based on the overexpression of ME, is effective to enhance D-lactate concentrations. We observed that the specific acetate yield peaked at 75 g-DCW/L condition, but the specific succinate yield was low at the high cell density. This might be explained by sensitivity for potassium ion on cell, since high concentration of potassium ion massively enhances level of succinate under dark anaerobic condition, probably in order to balance its ionic charge; on the other hand, the addition of potassium ion reduces acetate level[45]. The concentration of potassium ion would be a key determinant for secretion of various organic acids during autofermentation.

Importantly, the D-lactate was biosynthesized through photosynthesized glycogen metabolism. Optimization of initial cell concentration for autofermentation led to the highest reported D-lactate concentration of a photoautotrophic organism. In addition, the increased production of D-lactate (26.6 g/L) at high cell density (75 g-DCW/L) facilitates processes for recovering the product in high-yield. The present data could serve as a platform for metabolic engineering, leading to the large-scale production of D-lactate, thereby fulfilling the demand of the biorefinery sector.

Materials and Methods

Strains and culture conditions

Recombinant *Synechocystis* sp. PCC 6803 strains were inoculated to modified-BG11 medium containing 5 mM ammonium chloride and 50 mM Hepes-KOH, pH 7.8, in the presence or absence of 50 μg/mL kanamycin and/or 34 μg/mL chloramphenicol[20]. The cultivation proceeded at 30 °C under continuous light irradiation of 105~115 μmol/m^2/s photons and 1% (*v/v*) CO_2. Cell density was measured by optical density at 750 nm (OD_{750}). Dry cell weight (DCW) was measured after

harvesting of cells by filtration, followed by washing with 20 mM NH_4HCO_3, and lyophilization. All chemicals used were of analytical grade.

Construction of recombinant strains

The endogenous *me* (*slr0721*) gene was amplified from *Synechocystis* 6803 genomic DNA by PCR using the primer pair Slr0721-Fw and Slr0721-Rv. The primer sequences are listed in supplementary Table S1 in the Supporting Information. The amplified fragment was cloned into the *Nde*I/*Sal*I sites of the plasmid pSKtrc-slr0168[20], yielding pSKtrc-slr0168-12-slr0721. To construct a disruption vector for the *me* (*slr0721*) gene, a partial fragment of *me* was amplified from *Synechocystis* 6803 genomic DNA by PCR using the primer pair Slr0721Del-Fw and Slr0721Del-Rv and the resultant fragment was cloned into the *Sph*/*Sma*I sites of pUC119 (Takara Bio Inc., Shiga, Japan), yielding the plasmid pUC-Reg24. A kanamycin resistance gene cassette was amplified from the plasmid pTKP2031V[46] using the primer pair Kan-Fw and Kan-Rv and the amplified fragment was integrated into the *Msc*I site of pUC-Reg24 to yield pTKP0721. The D-lactate dehydrogenase gene (*ddh, slr1556*) was amplified from *Synechocystis* 6803 genomic DNA by PCR using the specific primer set Slr1556-Fw and Slr1556-Rv. The DNA fragment was integrated into the *Nde*I/*Bgl*II sites of pTCP1299-6803SigE[46] to yield the plasmid pTCP1299-slr1556. The principles underlying specific gene integration or disruption in *Synechocystis* sp. PCC6803 have been described previously[46]. The plasmids pSKtrc-slr0168-12-slr0721 and pSKtrc-slr0168 were used for gene integration in the host strain, *Synechocystis* sp. PCC6803 GT strain, to yield strains ME-ox and CT, respectively. The integration of each gene cassette was confirmed by PCR using the primer set Slr0168-Fw and Slr0168-Rv. The GT strain was transformed by pTKP0721 to disrupt the *me* gene through homologous recombination. The disruption of the *me* gene was analyzed by PCR using the primer set Slr0721-Fw2 and Slr0721Del-Rv. The ME-ox strain was transformed with the plasmid pTCP1299[46] to disrupt the *ackA* gene through homologous recombination. The resultant strain ME-ox/ΔackA was transformed with pTCP1299-slr1556 to integrate the *ddh* gene in the *ackA* gene loci, resulting in the strain ME-ox/ΔackA/ddh-ox (ME-ox, Δ*ackA*::*ddh*). The integration of gene fragments into the *ackA* gene loci was confirmed by PCR using the primer set Sll1299-Fw and Sll1299-Rv.

Organic acid production by fermentation

The recombinant *Synechocystis* sp. PCC 6803 strains were cultivated for 3 days at 30 °C under photoautotrophic conditions at an initial cell concentration of 0.1 g-DCW/L. The cultured cells were inoculated to 10 mL of 0.1 M Hepes-KOH (pH 7.8) containing 100 or 300 mM $NaHCO_3$ at initial cell concentrations of 5-7.5 g-DCW/L. Fermentation was conducted at 37 °C for 4 days under dark anoxic conditions (wrapped in foil and 100% N_2 bubbling). The accumulation of extracellular

organic acids during fermentation was quantified using a high-performance liquid chromatography (HPLC) system equipped with an Aminex HPX-87H column and an RID-10A refractive index detector. The HPLC system was operated at 50 °C using 5 mM H_2SO_4 at a flow rate of 0.6 mL min^{-1}. The glycogen concentration was determined by measuring the glucose released from glycogen by enzymatic hydrolysis as described previously[20]. The volumetric yield was calculated ratio of D-lactate amount to that of glucose consumed.

Analysis of intracellular metabolites

A 5 mg-DCW portion of cyanobacteria cells in the fermentation culture was collected at each sampling time (6, 24, 48, 72, and 96 h) by filtration using 1-μm pore size polytetrafluoroethylene (PTFE) disks (Millipore, Billerica, MA) and then immediately washed with 20 mM $(NH_4)_2CO_3$ pre-cooled to 4 °C. Intracellular metabolites were extracted and then analyzed with CE-MS (CE, Agilent G7100; MS, Agilent G6224AA LC/MSD TOF; Agilent Technologies, Palo Alto, CA) according to a previously reported method[20].

^{13}C-metabolic turnover analysis

^{13}C-labeling was initiated by the addition of 100 mM ^{13}C-sodium bicarbonate to the fermentation culture containing 100 mM Hepes-KOH buffer, pH 7.8. Culture samples were collected at the indicated time points (1, 2, 4, 6, 24, and 48 min) following the addition of ^{13}C-sodium bicarbonate. Each intracellular metabolite was extracted and then analyzed using CE-MS. Mass spectral peaks were identified by searching for mass shifts between the ^{12}C- to ^{13}C-mass spectra. The ^{13}C fractions, ratios of ^{13}C to total carbon, were calculated by relative isotopomer abundance of metabolites incorporating ^{13}C atoms, as described previously[20].

Enzyme assay

After 24 h fermentation under dark anoxic conditions, cells (100 mg-DCW) were collected by centrifugation at 6,000 × g for 10 min at 4 °C, washed in extraction buffer (18 mM KH_2PO_4, 27 mM Na_2HPO_4, 15 mM $MgCl_2$, and 100 μM EDTA; pH 6.8), suspended in 3 mL of the extraction buffer, and disrupted by sonication. After centrifugation at 20,000 × g for 20 min at 4 °C, the resulting supernatant was obtained as the crude extract. The D-lactate dehydrogenase assay was performed in 1.5 mL aliquots containing 100 mM potassium phosphate buffer (pH 7.5), 0.1 mM NADH, 1 mM sodium pyruvate and 75 μL of crude extract. D-Lactate dehydrogenase activity was determined by measuring NADH consumption as a change in A_{340}[21]. Protein levels were quantified using a QuantiPro™ BCA Assay Kit (Sigma-Aldrich, St. Louis, MO) according to the manufacturer's protocol. One unit was defined as the amount of enzyme that produced 1 μmol of NADH per min.

Supporting Information

Supplementary Table S1, Primers used in this study; Supplementary Figure S1, Targeted gene disruption by homologous recombination.

Acknowledgements

The authors thank Dr. Yuichi Kato and Ms. Ryoko Yamazaki for their technical assistance.

Funding Sources

This work was supported by the Advanced Low Carbon Technology Research and Development Program (ALCA) from the Japan Science and Technology Agency (JST), the Ministry of Education, Culture, Sports, Science, and Technology (MEXT), Japan.

Author Contributions

T.O. and T.H. designed the research. R.H. M.M. T.O. and T.H. analyzed the data and wrote the manuscript. A.K. supervised the study. All authors approved the final version of the manuscript.

Conflict of Interest: The authors declare that they have no conflicts of interest.

References

(1) Ostafinska, A., et al. (2017) Strong synergistic effects in PLA/PCL blends: Impact of PLA matrix viscosity. *J Mech Behav Biomed Mater*. 69, 229–241.

(2) Li, X., et al. (2017) *In vitro* degradation kinetics of pure PLA and Mg/PLA composite: Effects of immersion temperature and compression stress. *Acta Biomater*. 48, 468–478.

(3) Tsuji, H. (2005) Poly(lactide) stereocomplexes: formation, structure, properties, degradation, and applications. *Macromol Biosci.* 5, 569–597.

(4) Tsuji, H., Takai, H., and Saha, S. K. (2006) Isothermal and non-isothermal crystallization behavior of poly(l-lactic acid): Effects of stereocomplex as nucleating agent. *Polymer*. 47, 3826–3837.

(5) Mazzoli, R., Bosco, F., Mizrahi, I., Bayer, E. A. and Pessione, E. (2014) Towards lactic acid bacteria-based biorefineries. *Biotechnol Adv*. 32, 1216–1236.

(6) Poudel, P., Tashiro, Y. and Sakai, K. (2016) New application of *Bacillus* strains for optically pure L-lactic acid production: general overview and future prospects. *Biosci Biotechnol Biochem*. 80, 642–654.

(7) Dismukes, G.C., Carrieri, D., Bennette, N., Ananyev, G.M., and Posewitz, M.C. (2008) Aquatic phototrophs: efficient alternatives to land-based crops for biofuels. *Curr Opin Biotechnol*. 19, 235–240.

(8) Ho, S.H., Nakanishi, A., Kato, Y., Yamasaki, H., Chang, J.S., Misawa, N., Hirose, Y.,

Minagawa, J., Hasunuma, T., and Kondo, A. (2017) Dynamic metabolic profiling together with transcription analysis reveals salinity-induced starch-to-lipid biosynthesis in alga *Chlamydomonas* sp. JSC4. *Sci Rep*. 7, 45471.

(9) Wijffels, R.H., Kruse, O., and Hellingwerf, K.J. (2013) Potential of industrial biotechnology with cyanobacteria and eukaryotic microalgae. *Curr Opin Biotechnol*. 24, 405–413.

(10) Carroll A.L., Case A.E., Zhang, A., and Atsumi, S. (2018) Metabolic engineering tools in model cyanobacteria. *Metab Eng*. 50, 47–56.

(11) Kato, Y., Fujihara, Y., Vavricka, C.J., Chang, J.S., Hasunuma, T., and Kondo, A. (2019) Light/dark cycling causes delayed lipid accumulation and increased photoperiod-based biomass yield by altering metabolic flux in oleaginous *Chlamydomonas* sp. *Biotechnol Biofuels.* 21, 39.

(12) Angermayr, S.A., Gorchs Rovira, A., and Hellingwerf, K. J. (2015) Metabolic engineering of cyanobacteria for the synthesis of commodity products. *Trends Biotechnol*. 33, 352–361.

(13) Hasunuma, T., Matsuda, M., Senga, Y., Aikawa, S., Toyoshima, M., Shimakawa, G., Miyake, C., and Kondo, A. (2014) Overexpression of *flv3* improves photosynthesis in the cyanobacterium *Synechocystis sp.* PCC 6803 by enhancement of alternative electron flow. *Biotechnol Biofuel*. 7, 493.

(14) Lai, M.C., and Lan, E.I. (2015) Advances in metabolic engineering of cyanobacteria for photosynthetic biochemical production. *Metabolites.* 5, 636–658.

(15) Knoot, C.J., Ungerer, J., Wangikar, P.P., and Pakrasi, H.B. (2018) Cyanobacteria: Promising biocatalysts for sustainable chemical production. *J Biol Chem.* 293, 5044–5052.

(16) McNeely, K., Xu, Y., Bennette, N., Bryant, D.A., and Dismukes, G.C. (2010) Redirecting reductant flux into hydrogen production via metabolic engineering of fermentative carbon metabolism in a Cyanobacterium. *Appl Environ Microbiol*. 76, 5032–5038.

(17) Stal, L.J., and Moezalaar, R. (1997) Fermentation in cyanobacteria. *FEMS Microbiol Rev*. 21, 179–211.

(18) Osanai, T., Shirai, T., Iijima, H., Nakaya, Y., Okamoto, M., Kondo, A., and Hirai, M.Y. (2015) Genetic manipulation of a metabolic enzyme and a transcriptional regulator increasing succinate excretion from unicellular cyanobacterium. *Front Microbiol*. 6, 1064.

(19) Hasunuma, T., Harada, K., Miyazawa, S., Kondo, A., Fukusaki, E., and Miyake, C. (2010) Metabolic turnover analysis by a combination of *in vivo* ^{13}C-labelling from $^{13}CO_2$ and metabolic profiling with CE-MS/MS reveals rate-limiting steps of the C3 photosynthetic pathway in *Nicotiana tabacum* leaves. *J Exp Bot.* 61, 1041–1051.

(20) Hasunuma, T., Matsuda, M., and Kondo, A. (2016) Improved sugar-free succinate production by *Synechocystis* sp. PCC 6803 following identification of the limiting steps in glycogen catabolism. *Metab Eng Commun*. 3, 130–141.

(21) Ito, S., Takeya, M., and Osanai, T. (2017) Substrate specificity and allosteric regulation of a D-

lactate dehydrogenase from a unicellular cyanobacterium are altered by an amino acid substitution. *Sci Rep*. 7, 15052.

(22) Bricker, T.M., Zhang, S., Laborde, S.M., Mayer, P.R. 3rd., Frankel, L.K., Moroney, J.V. (2004) The malic enzyme is required for optimal photoautotrophic growth of *Synechocystis* sp. Strain PCC 6803 under continuous light but not under a diurnal light regimen. *J Bacteriol*. 186, 8144–8148.

(23) Williams, J.G.K. (1988) Construction of specific mutations in photosystem II photosynthetic reaction center by genetic engineering methods in *Synechocystis* 6803. *Methods Enzymol*. 167, 766–778.

(24) Yang, C., Hua, Q., and Shimizu, K. (2002) Metabolic flux analysis in *Synechocystis* using isotope distribution from ^{13}C-labeled glucose. *Metab Eng.* 4, 202–216.

(25) Young, J.D., Shastri, A.A., Stephanopoulos, G., and Morgan, J.A. (2011) Mapping photoautotrophic metabolism with isotopically nonstationary ^{13}C flux analysis. *Metab Eng.* 13, 656–665.

(26) Wan, N., DeLorenzo, D.M., He, L., You, L., Immethun, C.M., Wang, G., Baidoo, E.E.K., Hollinshead, W., Keasling, J.D., Moon, T.S., and Tang Y.J. (2017) Cyanobacterial carbon metabolism: Fluxome plasticity and oxygen dependence. *Biotechnol Bioeng*. 114, 1593–1602.

(27) Ito, S., Koyama, N., and Osanai, T. (2019) Citrate synthase from *Synechocystis* is a distinct class of bacterial citrate synthase. *Sci Rep.* 9, 6038.

(28) Knowles, V.L., Smith, C.S., Smith, C.R., and Plaxton, W.C. (2001) Structural and regulatory properties of pyruvate kinase from the Cyanobacterium *Synechococcus* PCC 6301. *J Biol Chem*. 276, 20966–20972.

(29) Camp, P.J., Miernyk, J.A., and Randall, D.D. (1988) Some kinetic and regulatory properties of the pea chloroplast pyruvate dehydrogenase complex. *Biochim Biophys Acta*. 933, 269–275.

(30) Wang, Q., Ingram, L.O., and Shanmugam, K.T. (2011) Evolution of D-lactate dehydrogenase activity from glycerol dehydrogenase and its utility for D-lactate production from lignocellulose. *Proc Natl Acad Sci USA*. 108, 18920–18925.

(31) Assavasirijinda, N., Ge, D., Yu, B., Xue, Y., and Ma, Y. (2016) Efficient fermentative production of polymer-grade D-lactate by an engineered alkaliphilic *Bacillus* sp. strain under non-sterile conditions. *Microb Cell Fact.* 15, 3.

(32) Awasthi, D., Wang, L., Rhee, M.S., Wang, Q., Chauliac, D., Ingram, L.O., Shanmugam, K.T. (2018) Metabolic engineering of *Bacillus subtilis* for production of D-lactic acid. *Biotechnol Bioeng*. 115, 453–463.

(33) Li, C., Tao, F., and Xu, P. (2016) Carbon flux trapping: Highly efficient production of polymer-grade D-lactic acid with a thermophilic D-lactate dehydrogenase. *Chembiochem*, 17, 1491–1494.

(34) Grabar, T. B., Zhou, S., Shanmugam, K. T., Yomano, L. P., and Ingram, L. O. (2006) Methylglyoxal bypass identified as source of chiral contamination in L(+) and D(−)-lactate fermentations by recombinant *Escherichia coli*. *Biotech Lett*. 28, 1527–1535.

(35) Ishida, N., Suzuki, T., Tokuhiro, K., Nagamori, E., Onishi, T., Saitoh, S., Kitamoto, K., and Takahashi, H. (2006) D-Lactic acid production by metabolically engineered *Saccharomyces cerevisiae*. *J Biosci Bioeng*. 101, 172–177.

(36) Zheng, H., Gong, J., Chen, T., Chen, X., and Zhao, X. (2010) Strain improvement of *Sporolactobacillus inulinus* ATCC 15538 for acid tolerance and production of D-lactic acid by genome shuffling. *Appl Microbiol Biotech.* 85, 1541–1549.

(37) Demirci, A., and Pometto, A. L. (1992) Enhanced production of D-lactic acid by mutants of *Lactobacillus delbrueckii*. *J Ind Microbiol.* 11, 23–28.

(38) Bustos, G., Moldesa, A. B., Alonsoa, J. L., and Vázquezb, M. (2004) Optimization of D-lactic acid production by *Lactobacillus coryniformis* using response surface methodology. *Food Microbiology.* 21, 143–148.

(39) Varman, A.M., Yu, Y., You, L., and Tang, Y.J. (2013) Photoautotrophic production of D-lactic acid in an engineered cyanobacterium. *Microbial Cell Fact*. 12, 117.

(40) Hollinshead, W.D., Varman, A.M., You, L., Hembree, Z., and Tang, Y.J. (2014) Boosting D-lactate production in engineered cyanobacteria using sterilized anaerobic digestion effluents. *Bioresour Technol.* 169, 462–467.

(41) Angermayr, S.A., van der Woude, A.D., Correddu, D., Kern, R., Hagemann, M., and Hellingwerf, K.J. (2016) Chirality matters: synthesis and consumption of the D-enantiomer of lactic acid by *Synechocystis* sp. strain PCC6803. *Appl Environ Microbiol.* 82, 1295–1304.

(42) Zhou, J., Zhang, H., Meng, H., Zhang, Y., and Li, Y. (2014) Production of optically pure D-lactate from CO_2 by blocking the PHB and acetate pathways and expressing D-lactate dehydrogenase in cyanobacterium *Synechocystis* sp. PCC 6803. *Process Biochem.* 49, 2071–2077.

(43) Hirokawa, Y., Goto, R., Umetani, Y., and Hanai, T. (2017) Construction of a novel D-lactate producing pathway from dihydroxyacetone phosphate of the Calvin cycle in cyanobacterium, *Synechococcus elongatus* PCC 7942. *J Biosci Bioeng*. 124, 54–61.

(44) Hasunuma, T., Matsuda, M., Kato, Y., Vavricka, C.J., and Kondo, A. (2018) Temperature enhanced succinate production concurrent with increased central metabolism turnover in the cyanobacterium *Synechocystis* sp. PCC 6803. *Metab Eng*. 48, 109–120.

(45) Ueda, S., Kawamura, Y., Iijima, H., Nakajima, M., Shirai, T., Okamoto, M., Kondo, A., Hirai, M.Y., and Osanai, T. (2016) Anionic metabolite biosynthesis enhanced by potassium under dark, anaerobic conditions in cyanobacteria. *Sci Rep*. 6, 32354.

(46) Osanai, T., Oikawa, A., Azuma, M., Tanaka, K., Saito, K., Hirai, M.Y., and Ikeuchi, M. (2011)

Genetic engineering of group 2 σ factor SigE widely activates expressions of sugar catabolic genes in *Synechocystis* species PCC 6803. *J Biol Chem*. 286, 30962–30971.

Figure legend

Fig. 1. Glycogen metabolic pathway to organic acids in *Synechocystis* 6803. Abbreviations: G6P, Glucose-6-phosphate; PEP, phosphoenolpyruvate; AcCoA, acetyl coenzyme A; Acetyl-P, acetyl-phosphate; ME, Malate dehydrogenase (decarboxylating); Ddh, D-lactate dehydrogenase.

Fig. 2. Extracellular organic acid content (D-lactate, succinate, and acetate) and intracellular glycogen in CT, ME-ox and ΔME cells after 96 h fermentation under dark anoxic conditions. Values represent the average (± standard deviation) of three independent experiments. Statistical significance was determined using the Tukey-Kramer test (*P < 0.05).

Fig. 3. Time-course changes of intracellular metabolite pool sizes in CT (black), ΔME (blue), and ME-ox (red) strains cultivated at 37 °C under dark anoxic conditions. Abbreviations: FBP, fructose 1,6-bisphosphate; F6P, fructose 6-phosphate; 3PGA, 3-phosphoglycerate. Values represent the average (± standard deviation) of three independent experiments.

Fig. 4. Time-course changes of ^{13}C fractions in metabolites initiated by the addition of ^{13}C-sodium bicarbonate in CT (black), ΔME (blue), and ME-ox (red) strains cultivated at 37 °C under dark anoxic conditions. Values represent the average (± standard deviation) of three independent experiments. Statistical significance was determined using the Tukey-Kramer test (*P < 0.01).

Fig. 5. Time-course changes of D-lactate, acetate, and succinate concentrations in ME-ox (red square), ME-ox/ΔackA (blue diamonds) and ME-ox/ΔackA/ddh-ox (green circles) cells at initial cell concentration of 5 g-DCW/L under dark anoxic fermentation in the presence of 300 mM $NaHCO_3$. Values represent the average (± standard deviation) of three independent experiments.

Fig. 6. Production of D-lactate, acetate and succinate in ME-ox/ΔackA/ddh-ox after 72 h fermentation in the presence of 100 mM $NaHCO_3$ in 100 mM Hepes-KOH (pH 7.5) at various initial cell concentrations (blue bar). Values represent the average (± standard deviation) of three independent experiments. Specific yield was calculated ratio of D-lactate production (g/L) to initial cell concentration (g-DCW/L) (Red bar).

Table 1. List of D-lactate bioproduction studies.

Organism	Conditions	D-Lactate titer (Cultivation time)	D-Lactate productivity	Reference
Escherichia coli strain TG114	Heterotrophic, glucose 120 g/L, 37°C	118 g/L (40 h)	2.88 g/L/h (0-40 h)	34
Synechocystis sp. PCC 6803	Mixotrophic with acetate, 30°C, +mutated *glyDH*	2.17 g/L (24 days)	0.0038 g/L/h (0-576 h)	39
Synechocystis sp. PCC 6803	Mixotrophic with acetate-rich anaerobic digestion effluents, 30°C, +mutated *glyDH*	1.2 g/L (20 days)	0.0025 g/L/h (0-480 h)	40
Synechocystis sp. Strain PCC6803,	Photoautotropic, 30°C, +*Lm*LdhD	0.35 g/L (14-day)	0.001 g/L/h (0-336 h)	41
Synechocystis sp. PCC6803	Dark anoxic, nitrogen- and phosphate-deprivation conditions, 30°C, Δ*phaCE*, Δ*pta*, +*ldhL*	1.06 g/L (4-days after fermentation)	0.011 g/L/h (0-96 h fermenation)	42
Synechococcus elongatus PCC7942	Photoautotrophic, 30°C, +*mgsA*, +*lldP*	1.23 g/L (24 days)	0.0021 g/L/h (0-576 h)	43
Synechocystis sp. PCC6803	Dark anoxic, Ppc-ox, Δ*ackA*, $NaHCO_3$, 37°C	10.7 g/L (3 days photoautotrophic growth and 3 days fermentation)	0.075 g/L/h (0-144 h)	44
Synechocystis sp. PCC6803	Dark anoxic, ME-ox, Δ*ackA*, +*ddh*, $NaHCO_3$,	26.6 g/L (3 days photoautotrophic	0.185 g/L/h (0-144 h)	This study

	37°C	growth and 3 days fermentation)

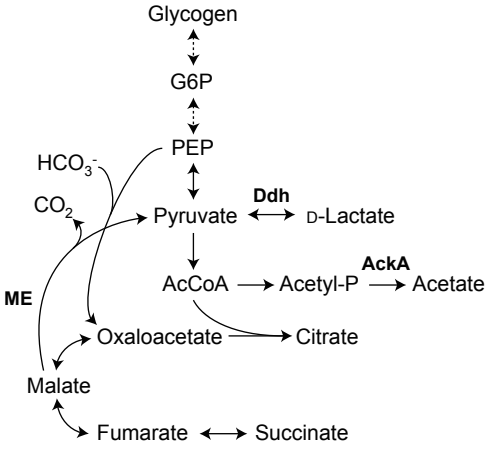
Glycogen
G6P
PEP
HCO_3^-
CO_2
Pyruvate
Ddh
D-Lactate
AcCoA
Acetyl-P
AckA
Acetate
ME
Oxaloacetate
Citrate
Malate
Fumarate
Succinate

Fig. 1

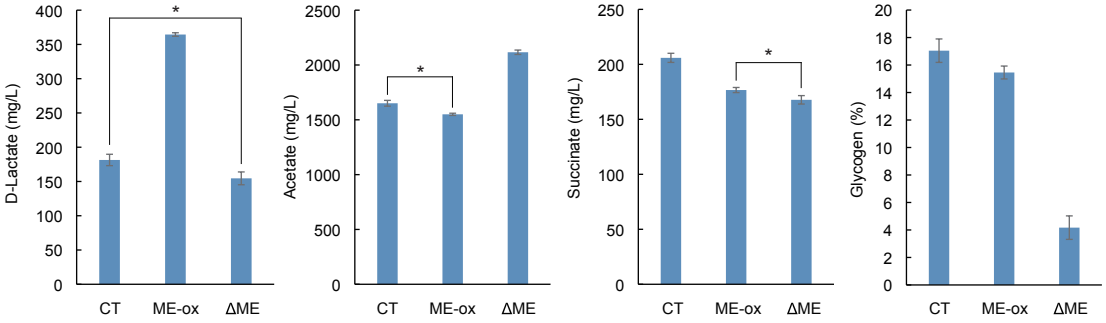
D-Lactate (mg/L)
400
350
300
250
200
150
100
50
0
*
CT
ME-ox
ΔME
Acetate (mg/L)
2500
2000
1500
1000
500
0
*
CT
ME-ox
ΔME
Succinate (mg/L)
250
200
150
100
50
0
*
CT
ME-ox
ΔME
Glycogen (%)
20
18
16
14
12
10
8
6
4
2
0
CT
ME-ox
ΔME

Fig. 2

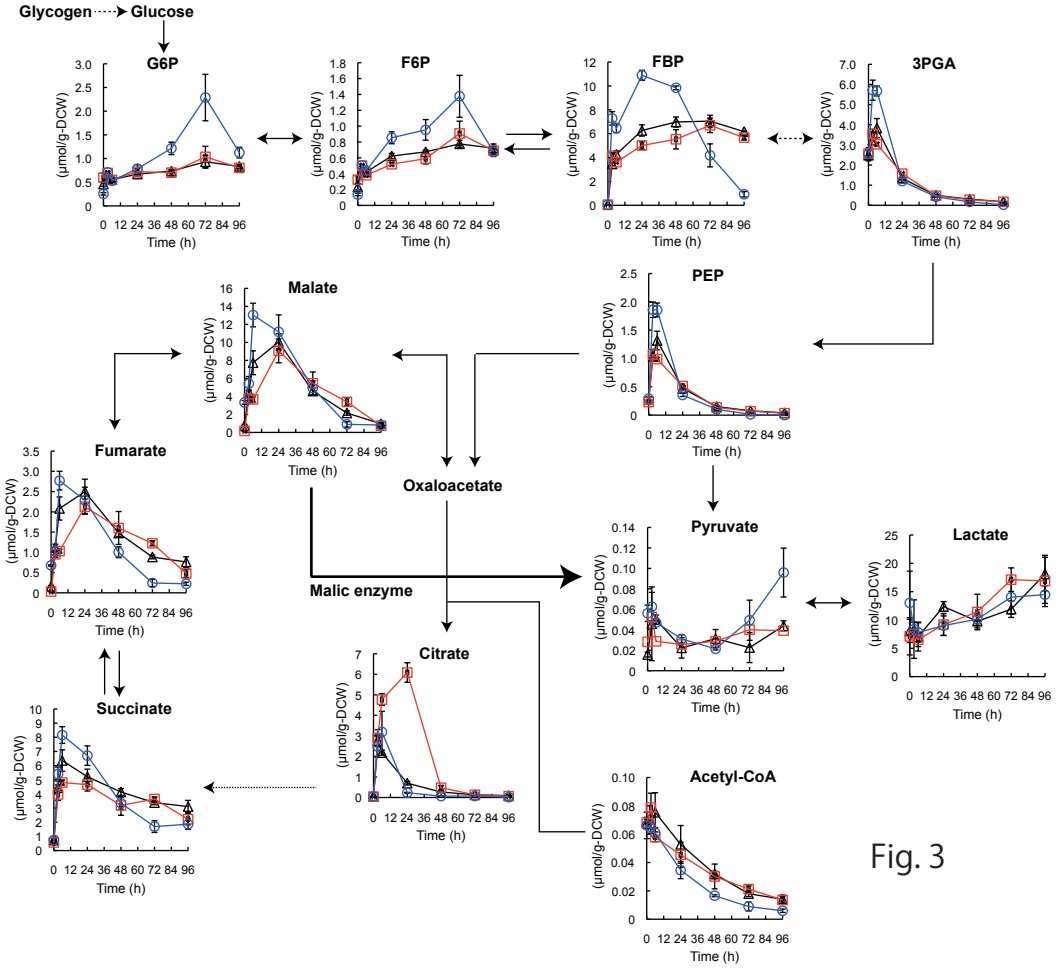
Glycogen
Glucose
G6P
F6P
FBP
3PGA
PEP
Malate
Fumarate
Oxaloacetate
Malic enzyme
Pyruvate
Lactate
Citrate
Succinate
Acetyl-CoA
(μmol/g-DCW)
Time (h)
0 12 24 36 48 60 72 84 96

Fig. 3

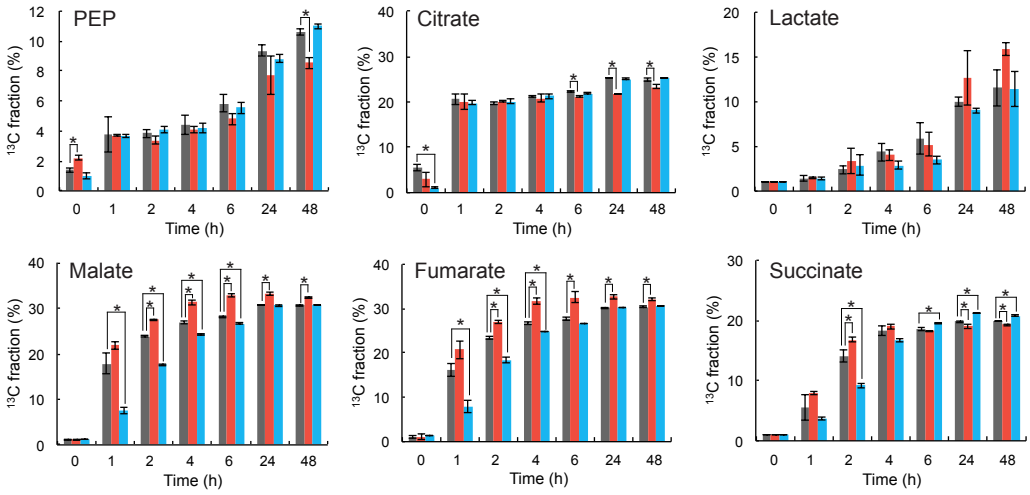
PEP
Citrate
Lactate
Malate
Fumarate
Succinate
^{13}C fraction (%)
Time (h)
0
1
2
4
6
24
48

Fig. 4

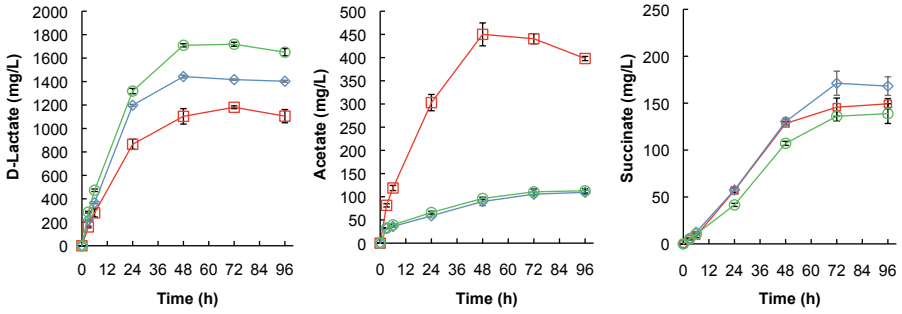
D-Lactate (mg/L)
2000
1800
1600
1400
1200
1000
800
600
400
200
0
0 12 24 36 48 60 72 84 96
Time (h)
Acetate (mg/L)
500
450
400
350
300
250
200
150
100
50
0
0 12 24 36 48 60 72 84 96
Time (h)
Succinate (mg/L)
250
200
150
100
50
0
0 12 24 36 48 60 72 84 96
Time (h)

Fig. 5

Fig. 6

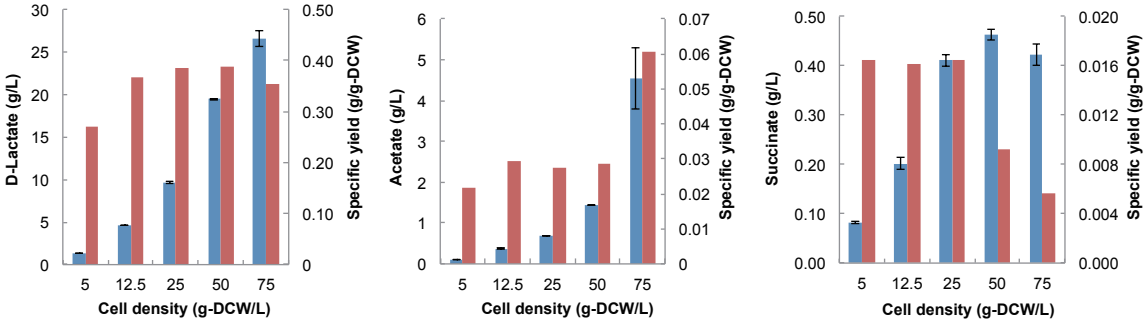
D-Lactate (g/L)
Specific yield (g/g-DCW)
Cell density (g-DCW/L)
5
12.5
25
50
75
Acetate (g/L)
Specific yield (g/g-DCW)
Cell density (g-DCW/L)
Succinate (g/L)
Specific yield (g/g-DCW)
Cell density (g-DCW/L)

Supporting Information

Malic enzyme facilitates D-lactate production through increased pyruvate supply during anoxic dark fermentation in *Synechocystis* sp. PCC 6803

Ryota Hidese[a], Mami Matsuda[a,b], Takashi Osanai[c], Tomohisa Hasunuma[a,b], and Akihiko Kondo[a,b,d].

[a]Graduate School of Science, Innovation and Technology, Kobe University, 1-1 Rokkodai, Nada, Kobe 657-8501, Japan. [b]Engineering Biology Research Center, Kobe University, 1-1 Rokkodai, Nada, Kobe 657-8501, Japan. [c]Department of Agricultural Chemistry School of Agriculture, Meiji University, 1-1-1 Higashimita, Tama-ku Kawasaki, Kanagawa, Japan. [d]Biomass Engineering Program, RIKEN, 1-7-22 Suehiro, Tsurumi, Yokohama, Kanagawa 230-0045, Japan

Supplementary Table S1. Primers used in this study.

Primer	Sequence (5′ to 3′)
Slr0721-Fw	AGGAAACAGACCCATATGGTTAGCCTCACCCCCAATC CGAG
Slr0721-Rv	CTGTAACCTGCAGGTCGACCTATTGACCGGCCACCCCT TCA
Slr0721Del-Fw	TTCCGCATGCCGAAGATCCGGAAAAGGT
Slr0721Del-Rv	TTAAGATATCAAAAACTTGGGCCGGGGC
Slr0721-Fw2	TGAGTGCGCCGGGGGTAGTGACCAAGG
Kan-Fw	TATTCTGGGCCCTTTGCTTCATCGCTCGAG
Kan-Rv	TATCAAGGGCCCATCCAATGTGAGGTTAAC
Slr1556-Fw	AAACCCAAGGGTTAACTTAATGGGGACAGATTACTTG GTAAGTTAAAG
Slr1556-Rv	AAGGAATTATAACCATATGAAAATCGCTTTTTTTAGCA GTAAAGCC
Slr0168-Fw	ATGGCACCGATGCGGAATCCCAACAGATTGCCTTTGAC
Slr0168-Rv	CACGTTGGGTCCCAAGTTTGTGCTGTGGCTGATGCCAT
Sll1299-Fw	TCAGCATTGATACCACTATGGGCTTCAC
Sll1299-Rv	GACAGCCCAGAGACTCCGAGCAAACCGGA

Supplementary Fig. S1. Targeted gene disruption by homologous recombination. (A) The CT, ME-ox, ΔME strains were separately created from the parental strain *Synechocystis* 6803 GT by homologous recombination. The *ackA* gene was deleted from the genome of the ME-ox strain, and then the *ddh* gene was introduced to the resulting ME-ox/ΔackA strain, yielding the ME-ox/ΔackA/ddh-ox strain. Integration or disruption was confirmed by PCR, and the positions of the primer-annealing sites for PCR are indicated by arrows. Abbreviations: K_m^r, kanamycin resistance gene; P_{trc}, *trc* promoter; P_{psbA2}, *psbA2* promoter; *Chl*^{r}, chloramphenicol resistance gene. (B) PCR analysis of the DNA region containing each gene cassette in the parental GT strain and each recombinant strain. The sizes of PCR fragments obtained from the corresponding primer pairs are shown in (A). DNA size markers are shown in lane M.

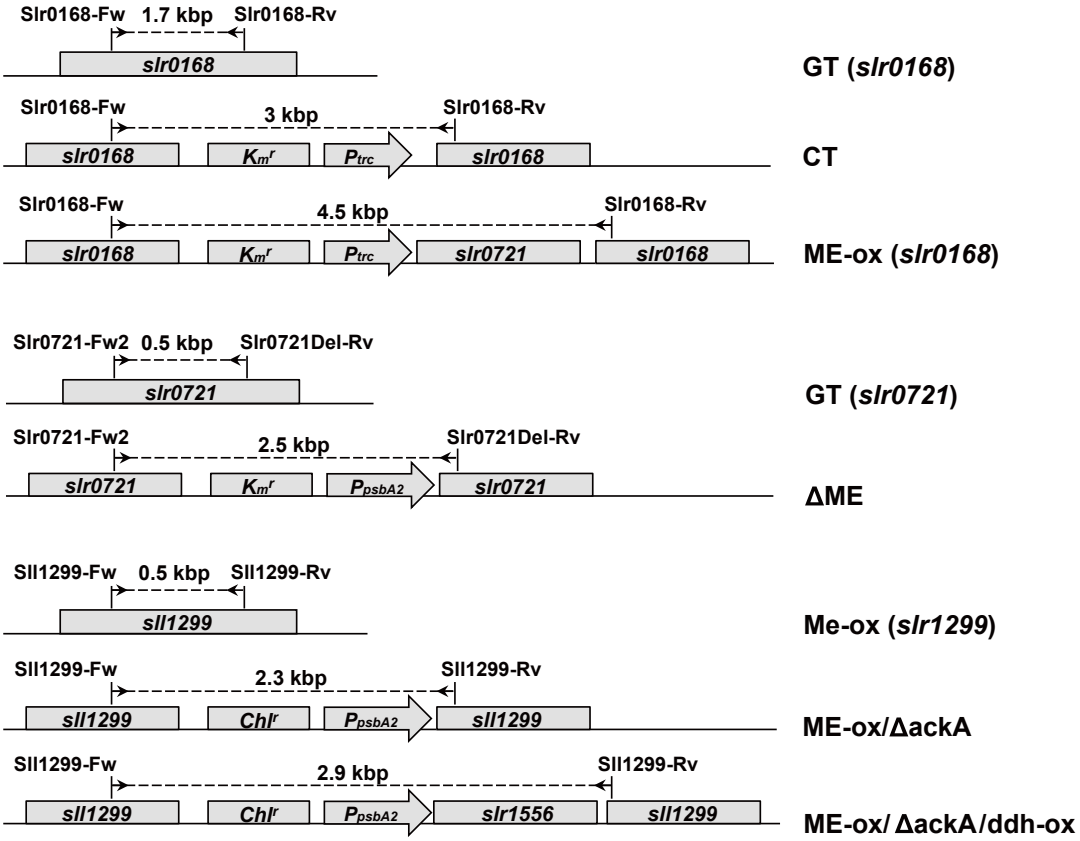

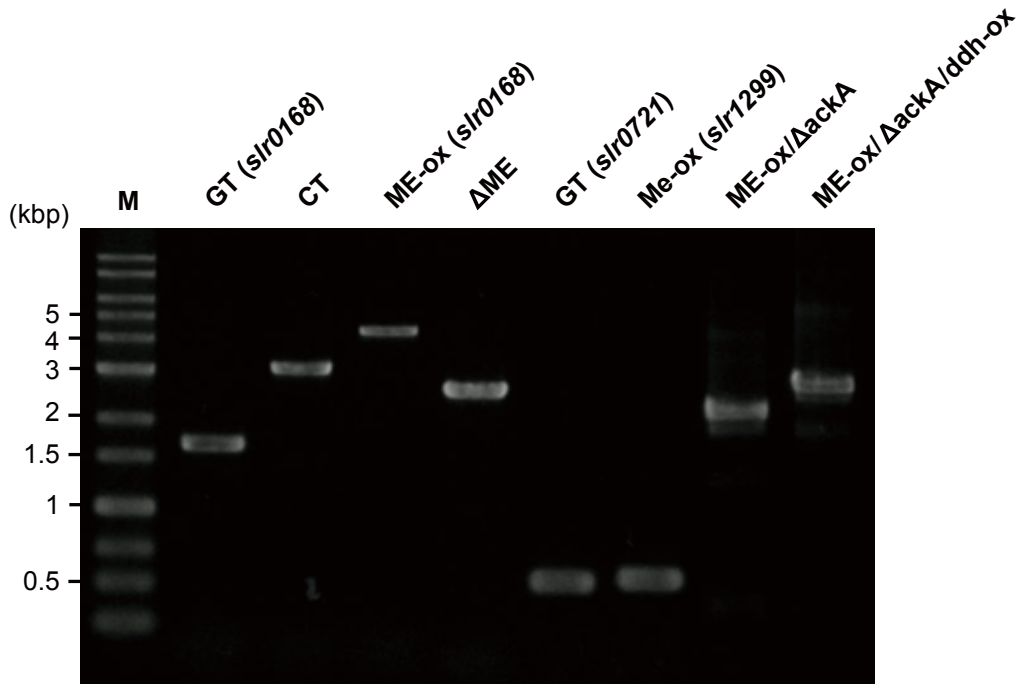

Fig S1. Targeted gene disruption by homologous recombination.